ahydrate appeared to be the predominant species in most of the solid products.

Discussion

These bench-scale experiments indicate that use of a method which combines spray absorption with magnesia scrubbing can remove greater than 90% of the SO_2 from gas streams containing 0.1–1.0% SO_2 under controlled conditions. The resulting product will probably be a mixture of $MgSO_3 \cdot 3H_2O$ and $MgSO_3 \cdot 6H_2O$, with the hexahydrate predominating at lower temperatures and higher humidities. Hexahydrate formation is also favored at lower temperatures in wet magnesia scrubbers (Lowell et al., 1977). The magnesium sulfite hydrates can be dehydrated and subsequently decomposed thermally to provide MgO for recycle to the scrubber and to generate a concentrated SO_2 gas stream which can be used for sulfuric acid or sulfur production (Lowell et al., 1976). Thermogravimetric studies verified that the magnesium sulfite hexahydrate can be dehydrated at temperatures up to 250 °C without significant decomposition to SO_2. The temperature range for the decomposition to MgO and SO_2 is 400–800 °C.

Before such an FGD system could be utilized under processing conditions, it would be necessary to further define the effects of process contaminants and other gases such as oxygen and carbon dioxide on the efficiency and recycle characteristics of the system. The presence of carbon dioxide would result in the formation of magnesium carbonate, which could be decomposed thermally to regenerate MgO. Partial oxidation to sulfate has been reported when the scrubbed gases contain oxygen (Blythe et al., 1983). This product could not be readily decomposed to MgO for recycle. Additional studies would be needed to determine conditions which would decrease sulfate formation. In the lime system, contaminants such as fly ash and HCl are not as important because the product is discarded. The magnesia system, on the other hand, is regenerable; thus, contaminants in the solid product would accumulate during recycle and could eventually pose significant problems. It is expected that some of these potential problems could be minimized through the use of a prescrubber and particulate precipitators upstream of the spray absorber. Remaining contaminants could be removed by a small purge stream from the recycle loop.

Acknowledgment

We thank S. P. N. Singh and J. E. Mrochek for technical review, M. G. Stewart for editorial assistance, and D. J. Weaver for manuscript preparation. This research was sponsored by the Morgantown Energy Technology Center, US Department of Energy, under Contract DE-AC0584OR21400 with Martin Marietta Energy Systems, Inc. Part of this work was presented at the 183rd National American Chemical Society Meeting, Las Vegas, NV, 1982.

Registry No. MgO, 1309-48-4; $MgSO_3 \cdot 3H_2O$, 19086-20-5; $MgSO_3 \cdot 6H_2O$, 13446-29-2; SO_2, 7446-09-5.

Literature Cited

Ayer, F. A., "Proceedings, Symposium on Flue Gas Desulfurization, Houston, October 1980"; 2 Vols. April 1981; EPA-600/9-81-019.

Blythe, G. M.; Burke, J. M.; Kelly, M. E.; Rohlack, L. A.; Rhudy, R. G. In "Proceedings: Symposium on Flue Gas Desulfurization, Hollywood, Florida, May 1982"; Ayer, F. A., Ed.; March 1983; EPRI-CS-2897, Vol. II, p 595.

Burnett, T. A.; Wells, W. L. In "Flue Gas Desulfurization"; Hudson, J. L., Rochelle, G. T., Eds.; American Chemical Society: Washington, DC, 1982; p 381.

Gille, J. A.; MacKenzie, J. S. In "Proceedings, Symposium on Flue Gas Desulfurization, Hollywood, Florida, Nov 1977"; March 1978; EPA-600/7-78-058b, p 737.

Koehler, G. R. *Chem. Eng. Prog.* **1974**, *70*, 63.

Lowell, P. S.; Meserole, F. B.; Parsons, T. B. "Precipitation Chemistry of Magnesium Sulfite Hydrates in Magnesium Oxide Scrubbing"; Sept 1977; EPA-600/7-77-109.

Lowell, P. S.; Corbett, W. E.; Brown, G. D.; Wilde, K. A. "Feasibility of Producing Elemental Sulfur from Magnesium Sulfite"; Oct 1976, EPA-600/7-76-030.

Martin, J. R.; Ferguson, W. B.; Frebotta, D. *Combustion* **1981**, *52*, 12.

Meyler, J. *Combustion* **1981**, *52*, 21.

Rochelle, G. T. "Process Synthesis and Innovation in Flue Gas Desulfurization"; July 1977; EPRI FP-463-SR.

Satriana, M., Ed. "New Developments in Flue Gas Desulfurization Technology"; Noyes Data Corp.: Park Ridge, NJ, 1981.

Taylor, R. B.; Gambarani, P. R.; Erdman, D. In "Proceedings: Symposium on Flue Gas Desulfurization, New Orleans, March 1976"; May 1976; EPA-600/2-76-136B, Vol. II, p 735.

Received for review May 20, 1985
Revised manuscript received October 24, 1985
Accepted November 1, 1985

Weeping from Sieve Trays

M. J. Lockett*† and S. Banik‡

Department of Chemical Engineering, UMIST, Manchester, U.K.

A comprehensive study has been made on the rates of liquid weeping from sieve trays in a hydraulic simulator. Results are reported both for air–water and air–Isopar M. A wide range of tray geometries and flow rates was used. The influence on the weep rate of individual parameters such as hole gas velocity, liquid rate, weir height, hole diameter, and fractional perforation area is discussed. The results have been correlated by expressing the weep flux as a function of the Froude number.

For years, it has been common practice to consider the weep point as the lower limit of satisfactory operation of a distillation tray, but recent studies (Lockett et al., 1984; Brambilla et al., 1979) have indicated that trays can operate below the weep point without incurring a substantial loss of efficiency. To operate a tray confidently below the weep point, it is necessary to be able to predict the weeping rate together with the effect on efficiency.

Some weep rate data are available in the open literature (Brown, 1958; Wada et al., 1966; Lemieux and Scotti, 1969; Zenz et al., 1967; Nutter, 1972; Koziol and Koch, 1976; Nutter, 1979; Zhou et al., 1980). These are mostly based

* To whom correspondence should be addressed.
† Present address: Union Carbide Corp., Tonawanda, NY 14151-0044.
‡ Present address: Engineers India Ltd., New Delhi—110001, India.

0196-4305/86/1125-0561$01.50/0

Table I. Tray Details

tray	A	B	C	D	E	chimney
hole diameter, mm	12.7	12.7	12.7	6.4	3.2	50
hole pitch, mm	39	32	25	19	10	
no. of holes	328	493	662	1292	5280	16
% free area	10.2	15.0	20.0	10.2	10.2	
thickness, mm	3	3	3	3	3	

[a] Sharp edge of holes facing gas flow, clearance under downcomer = 25–50 mm, 25-mm inlet weir used when liquid load ≤15 $m^3/(m\ h)$.

on small diameter columns operating at low liquid rates. Weep rate correlations have been given by Wada et al. (1966) for 3 mm hole sieve trays and by Zenz et al. (1967) for 1.6–6.4 mm hole trays, but again the latter was developed by using data from a small column. In small columns, with liquid flow path lengths of perhaps less than 0.5 m, tray hydrodynamic behavior tends to be dominated by liquid entry and exit conditions so that the results are unrepresentative of those obtained from a larger tray.

In the present study, weeping rates were measured by using a somewhat larger column, and a very large range of variables was studied. In addition, under certain conditions, weeping was found to be nonuniformly distributed over the tray, and an attempt has been made to study the relative rates of weeping from the two halves of the tray. Although the present results were obtained by using a rectangular tray, they are expected to be valid for predicting weeping rates from trays in round columns, providing the column diameter is greater than about 1.2 m (Colwell, 1979).

Experimental Work

Figure 1 shows a schematic representation of the column used for the study. It consisted of a rectangular column of dimensions 1.22 m × 0.63 m containing four sieve trays and a chimney tray. The column had glass walls to facilitate the observation of the froth on the trays. The chimney tray was located below the test tray, as shown in Figure 1, and it collected liquid which wept from the test tray. Weeping liquid flowed from the chimney tray, through a rotameter, and was returned to the liquid storage vessel. The same tray spacing (0.41 m) was used between all trays including the chimney tray. A transverse baffle was included on the chimney tray to enable weeping from each half of the test tray to be measured. Dry tray pressure drops were measured by blocking off the clearance under the downcomers.

Details of the stainless steel trays which were used are given in Table I. Further details have been given previously (Lockett, 1981). Particular care was taken to ensure that the trays were level. The air velocity profile below the test tray was measured by a Pitot tube to confirm that the air flow to the test tray was uniform. The systems used were air–water and air–Isopar M. The relevant properties of Isopar M are as follows: density, 780 kg/m^3; surface tension, 23 mN/m; viscosity, 2.4 m N s/m^2; flashpoint 78 °C. As far as possible, the experiments were conducted to study one variable at a time. The effect of the following variables on the weeping rate was studied: gas flow rate, hole diameter, liquid flow rate, percentage perforated area; weir height, and liquid physical properties. The clear-liquid height profile from weir to weir across the test tray was obtained from the dynamic liquid head, which was measured by using a series of manometers set in the tray floor along the center line of the tray.

A parallel study was also carried out on a valve tray which is not reported here (Banik, 1982).

Reproducibility of Results. Some of the experimental runs were repeated after an interval of 9 months, during which time a number of tray changes had been made.

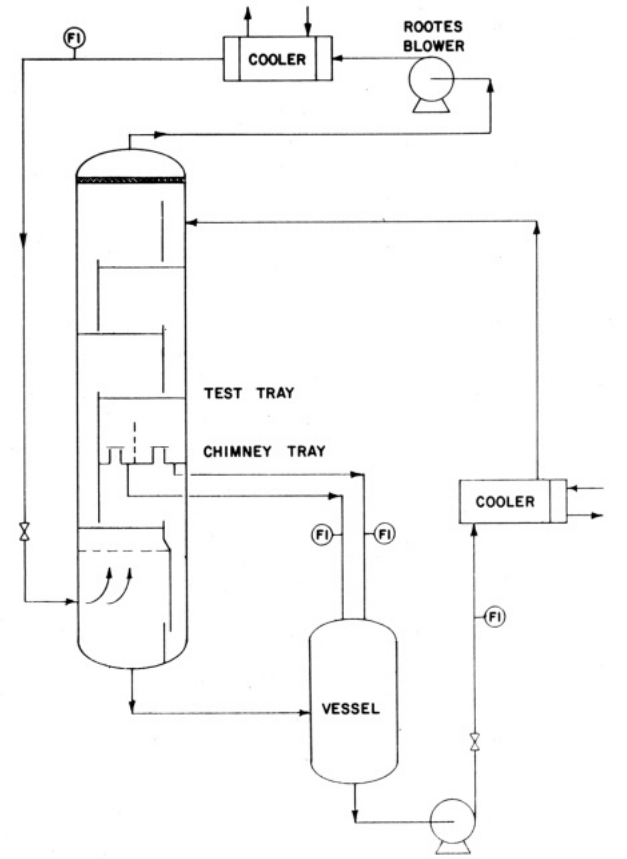

Figure 1. Schematic flow sheet.

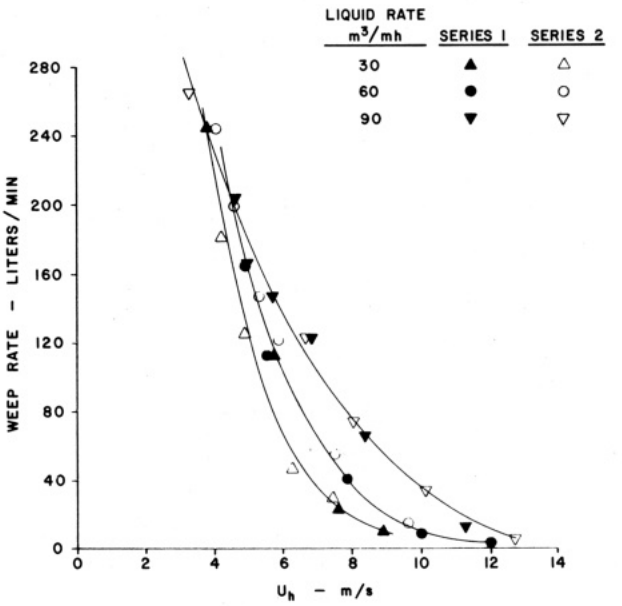

Figure 2. Reproducibility of experimental data: tray A, weir = 50 mm, air–water.

Some of the results are shown in Figure 2, and they serve to confirm that reproducible measurements of the weeping rate were being made.

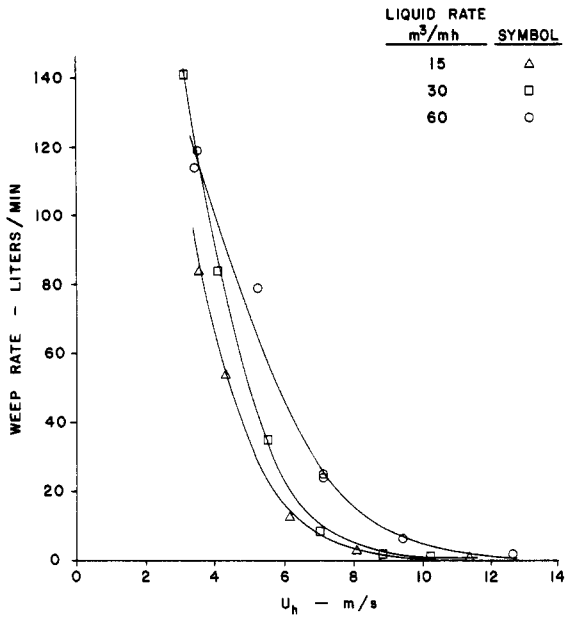

Figure 3. Effect of liquid flow rate: tray A, weir = 25 mm, air–Isopar M.

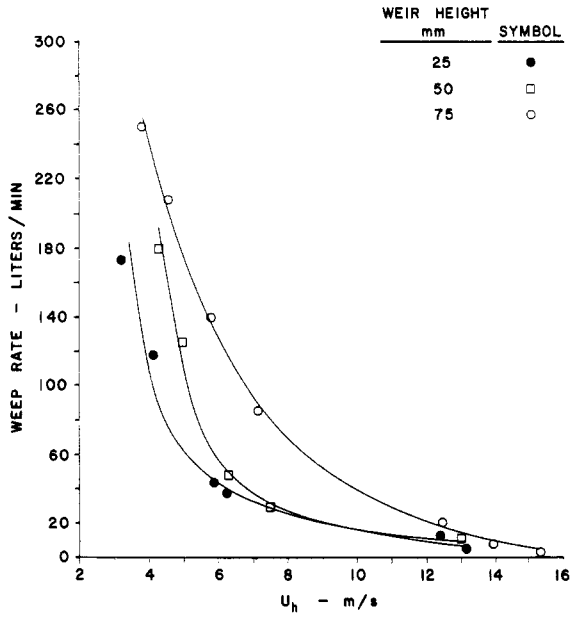

Figure 4. Effect of weir height: tray A, liquid rate = 30 $m^3/(m\ h)$, air–water.

Experimental Results

A very large amount of data was generated, but it is impractical to report all of it here. In what follows, we report the general trends of our results. More comprehensive results have been given by Banik (1982).

Liquid Flow Rate. Apart from demonstrating reproducibility, Figure 2 also shows typical behavior with respect to liquid flow rate. An increase of the liquid rate increases the clear-liquid height on the tray and generally leads to an increase in the weeping rate. Figure 2 refers to air–water, and a similar effect is shown in Figure 3 for the air–Isopar M system.

Weir Height. In general, increasing the weir height leads to an increase in the clear-liquid height and to an increase in the weeping rate as shown in Figure 4. At very high liquid rates, however, it was found that a change of the weir height from 50 to 75 mm had only a small effect—Figure 5. Some rather unusual behavior was observed when using a combination of low weir height (25 mm) and high liquid load (60–90 $m^3\ m^{-1}\ h^{-1}$). Under these circumstances, weeping tended to be lower than expected, and it may be that this is attributable to the high horizontal velocity of the liquid crossing the tray.

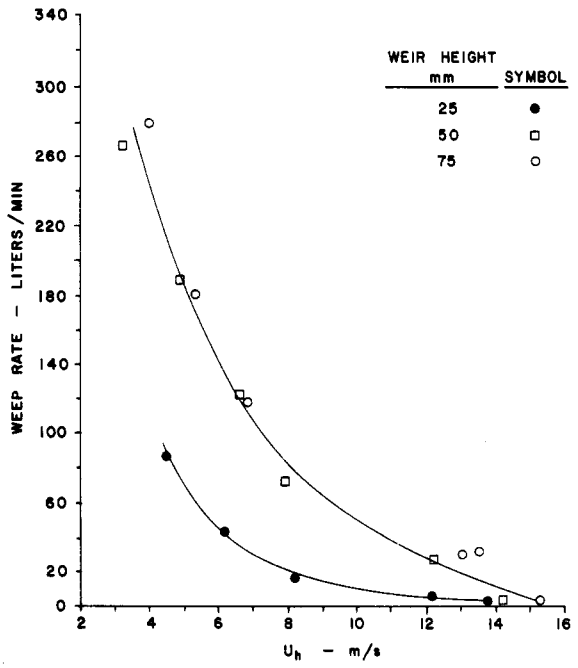

Figure 5. Effect of weir height at high liquid rate: tray A, liquid rate = 90 $m^3/(m\ h)$, air–water.

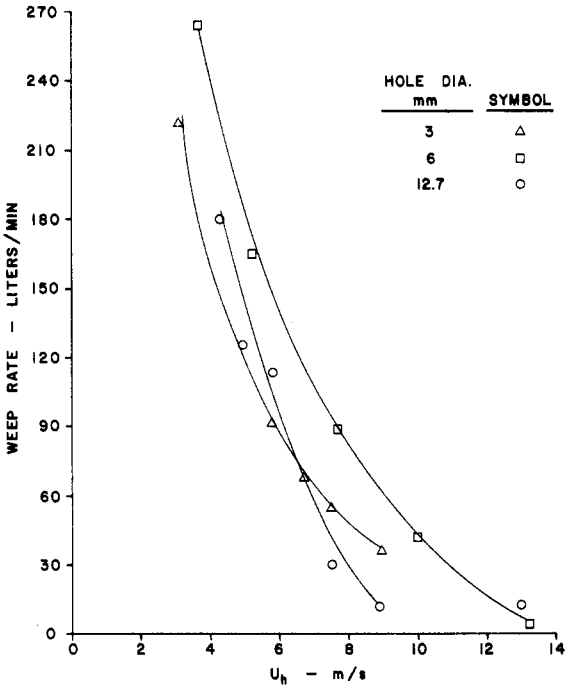

Figure 6. Effect of hole diameter: trays A, D, and E, liquid rate = 30 $m^3/(m\ h)$, air–water, weir = 50 mm.

Hole Diameter. The effect of the hole diameter on the weeping rate gave results which were the most unexpected of those we obtained. It was found that the weeping rate was a maximum for 6.4 mm diameter holes with 3- and 12.7-mm holes both showing a lower weeping rate. Figure 6 shows results typical of those obtained. The maximum weeping rate from 6.4-mm holes was found to be quite reproducible and to persist over a range of liquid flow rates from 15 to 90 $m^3\ m^{-1}\ h^{-1}$. Our interpretation of this is based on visual observations of the underside of the tray

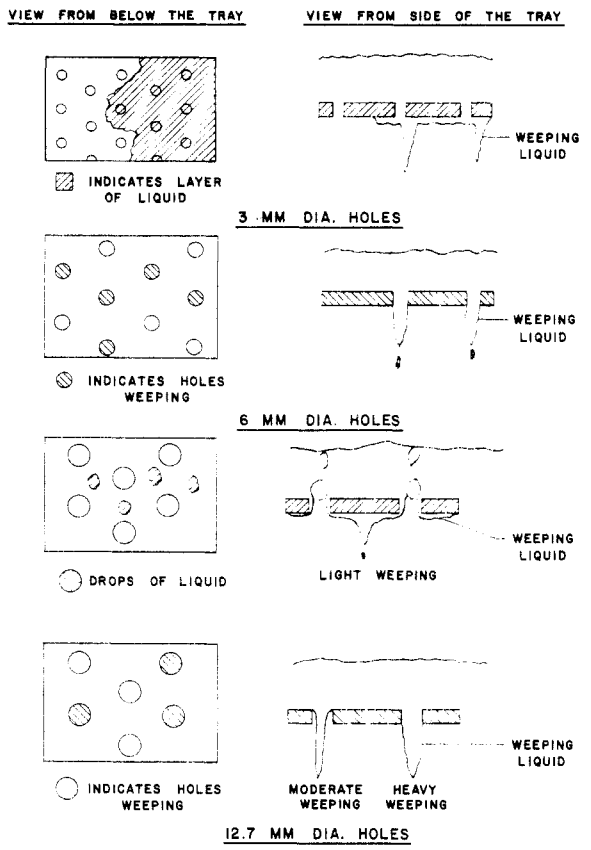

Figure 7. Representation of mechanisms of weeping from sieve trays.

during weeping. It was observed that weeping appeared to occur by a different mechanism for the three different hole diameters studied. Figure 7 shows a schematic representation of the behavior observed for 3, 6.4, and 12.7 mm diameter holes using the air–water system. It was found that the 3-mm holes exhibited severe bridging of the liquid under the tray. A layer of liquid covered the underside of the tray, and the weeping liquid disengaged as streams from this layer. The number of streams was substantially less than the number of holes in a given area.

For the 6.4-mm holes, the weeping liquid disengaged from the holes as jets irrespective of the weep rate. This behavior apparently is responsible for the high weeping rates observed.

The mechanism of weeping from 12.7-mm holes changed depending on the weep rate (or the gas velocity). At low weeping rates, a layer of liquid covered the underside of the tray from which weeping occurred. At higher weeping rates, weeping took place directly from the holes. At medium weeping rates, the jet diameter was less than the hole diameter, and at the highest weeping rates, it filled the hole. At the present time, we have no clear understanding about when and why these different mechanisms occur. Furthermore, it is possible that the behavior may depend on the surface tension, and all these experiments with differing hole diameters were carried out with air–water. Nevertheless, we believe these observations to be interesting, and the maximum weeping rates from 6.4-mm holes seem to be related to this observed behavior.

Percentage Free Area. At a given hole gas velocity, the weeping rate increases with increasing percentage free area of the tray—Figure 8. When the weeping rate is expressed as a weep flux based on the open area of the tray, the difference between the two trays of different percent free areas is much reduced, Figure 9. In fact, we do not expect to entirely reconcile the behavior of trays of differing free areas in this way because at the same hole gas velocity, the superficial gas velocities are greatly different. Consequently, the clear-liquid heights on the two trays are different which will have an influence on the weeping rates. Nevertheless, expressing the weep rates in terms of a weep flux in this way seems a promising first step in reconciling data from trays of different free areas. It is worth noting that this same approach was also used by Zenz et al. (1967). Another difficulty is that froth heights and weeping rates were noticeably more nonuniform using the larger percentage free area of the tray.

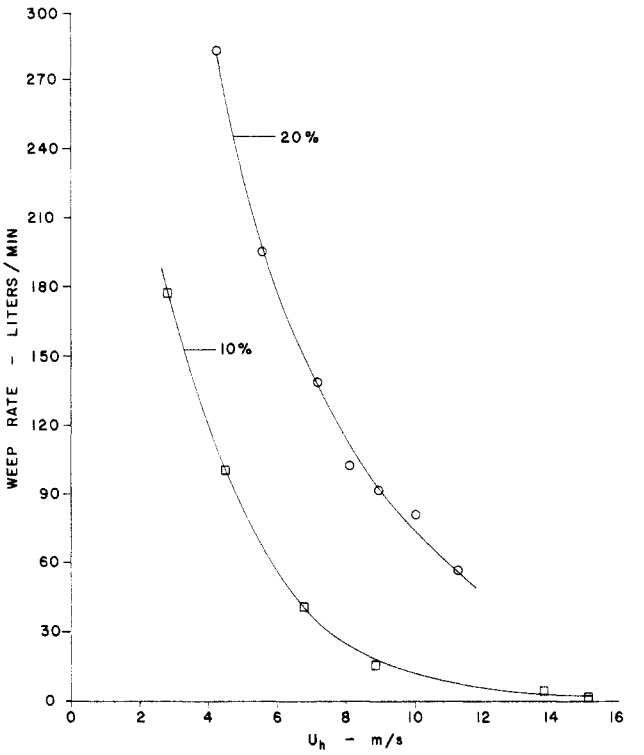

Figure 8. Effect of percentage hole area: trays A and C, liquid rate = 60 $m^3/(m\ h)$, air–water, weir = 25 mm.

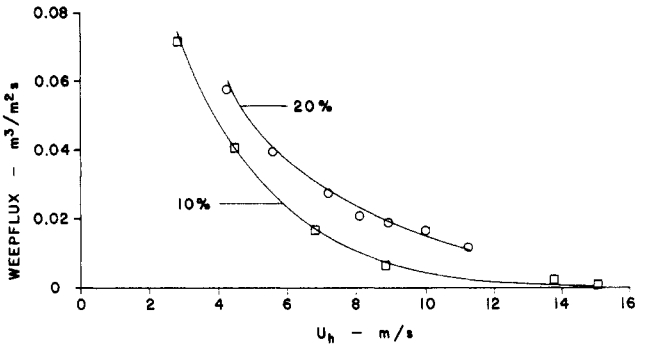

Figure 9. Weep flux vs. gas hole velocity: trays A and C, liquid rate = 60 $m^3/(m\ h)$, air–water, weir = 25 mm.

Liquid Physical Properties. In general, little difference was found in the rates of weeping using the air–water and the air–Isopar M systems. Figure 10 shows a typical difference between the two systems. The slightly higher weeping rate using water may be attributable to its slightly higher density. It is unlikely that differences in the surface tension play any significant role with 12.7 mm diameter holes.

Nonuniformity of Weeping. The results discussed above are all in terms of the total weeping rate from the tray. However, weeping rates were also measured from each half of the tray—the half near the liquid inlet and the half near the exit weir.

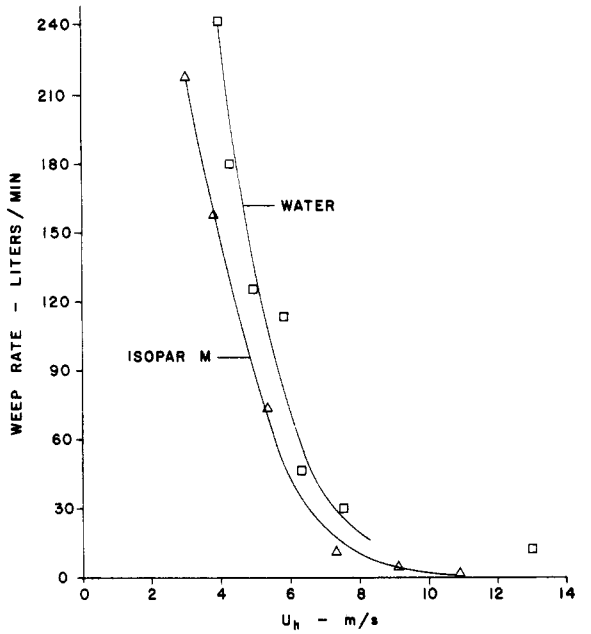

Figure 10. Comparison of weeping behavior using water (□) and Isopar M (△): tray A, liquid rate = 30 $m^3/(m\ h)$, weir = 50 mm.

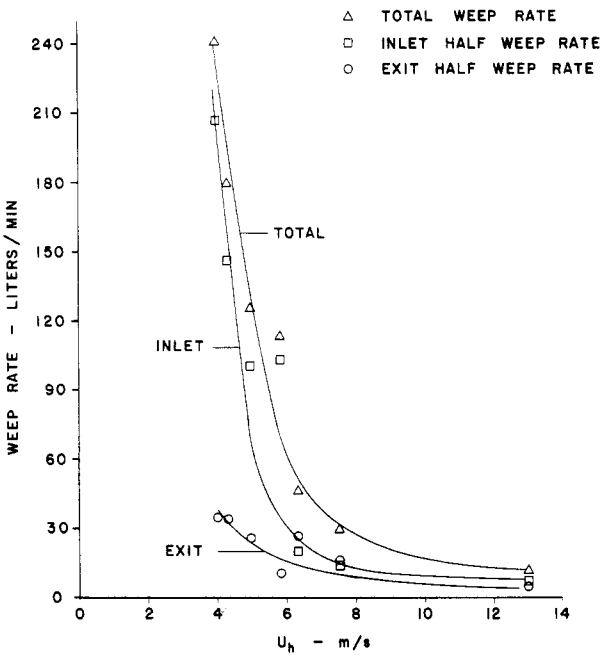

Figure 11. Showing weeping mainly from inlet half of the tray: tray A, liquid rate = 30 $m^3/(m\ h)$, air–water, weir = 50 mm.

In general, it was found that weeping was not uniformly distributed over the tray and an excess of weeping could occur over the inlet half or over the exit half depending on the conditions which prevailed. Figure 11 shows a case where weeping was mainly from the inlet half of the tray. At a higher liquid rate, the situation reversed and the weeping occurred mainly from the exit half of the tray—Figure 12. In both cases, the total rate of weeping was similar. These differences are important since weeping from the inlet half has a more serious effect on tray efficiency than weeping from the exit half. Theoretical analysis of this has been completed (Banik, 1982) and will be published at a later date. In some cases, weeping is more nearly uniform, and Figure 13 shows such a case. On the basis of our data, a tentative regime map is shown in Figure 14. No attempt has been made to include boundaries on Figure 14. One reason for the behavior

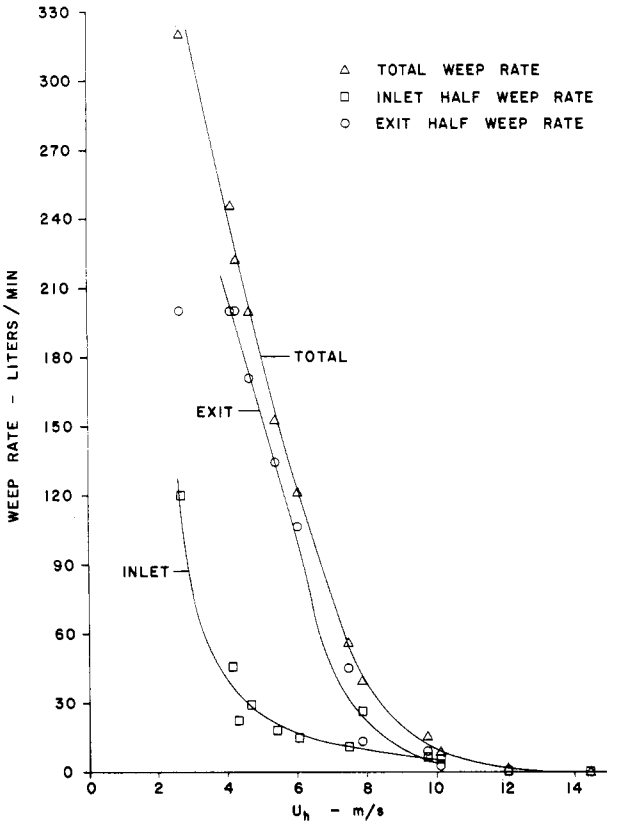

Figure 12. Showing weeping mainly from exit half of the tray: tray A, liquid rate = 60 $m^3/(m\ h)$, air–water, weir = 50 mm.

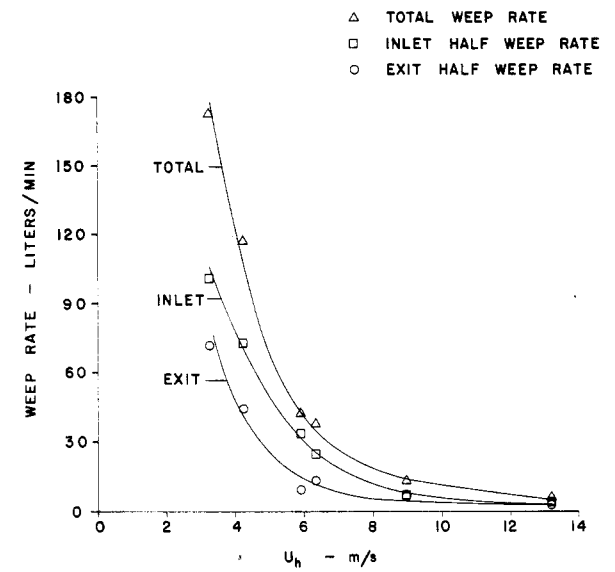

Figure 13. Showing a case of relatively uniform weeping: tray A, liquid rate = 30 $m^3/(m\ h)$, air–water, weir = 25 mm.

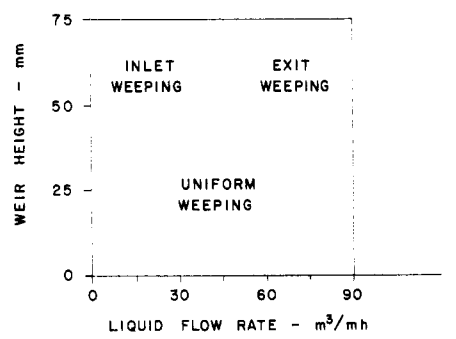

Figure 14. "Regime map" for nonuniform weeping: tray A.

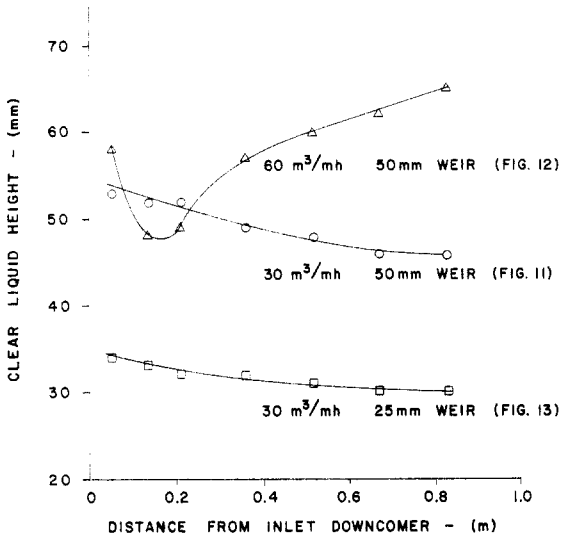

Figure 15. Clear-liquid height profiles: tray A, U_h = 4.3 m s^{-1}.

described is believed to be the presence of a hydraulic jump at high liquid loads which suppresses the liquid weeping near the inlet and accentuates it near the exit. Some indication of this behavior can be found in the measured clear liquid height profiles corresponding to Figures 11–13 which are shown in Figure 15. The importance of this is likely to depend on the tray dimensions. The subject of nonuniform weeping is extremely complex and is worth studying further as a function of the tray diameter.

Weep Rate Correlation

An analysis of the correlations proposed for predicting the weep point indicated that the most important parameter is the Froude number based on the hole gas velocity where

$$Fr = U_h\left(\frac{\rho_G}{gh_{CL}\rho_L}\right)^{0.5} \tag{1}$$

Now the dry tray pressure drop can be written as

$$\Delta P_d = \xi\rho_G U_h^2/2g\rho_L \tag{2}$$

where typically $\xi \simeq 2$, so that

$$Fr = \left(\frac{\Delta P_d}{h_{CL}}\right)^{0.5} \tag{3}$$

From this, the significance of the Froude number in determining the weeping may be understood. It represents the ratio between the dry tray pressure drop which tends to prevent weeping and the clear-liquid height which tends to cause weeping.

Based on this, admittedly rather simple, analysis, we have attempted to correlate our weeping data by plotting the weep flux vs. Fr^{-1}. The weep flux (WF) is defined as

$$WF = \frac{\text{weep rate (m}^3\text{ s}^{-1})}{\text{hole area (m}^2)} \tag{4}$$

The clear-liquid height was estimated from

$$h_{CL} = \Delta P_T - \Delta P_d \tag{5}$$

where ΔP_T is the measured tray pressure drop and ΔP_d is the measured dry tray pressure drop at the same gas velocity. It was found that inclusion of additional terms in (5) to allow for the residual pressure drop or surface tension head loss made no significant difference to the correlation.

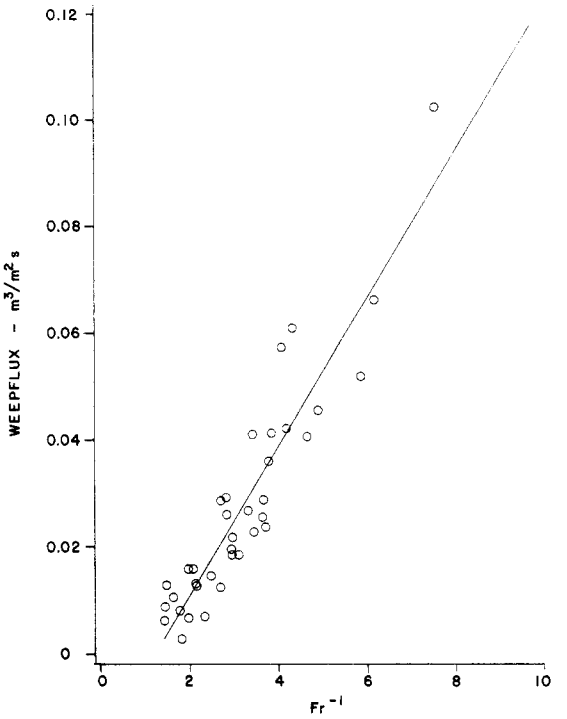

Figure 16. Correlation of results for tray E (3.2-mm holes, 10.2%): air–water.

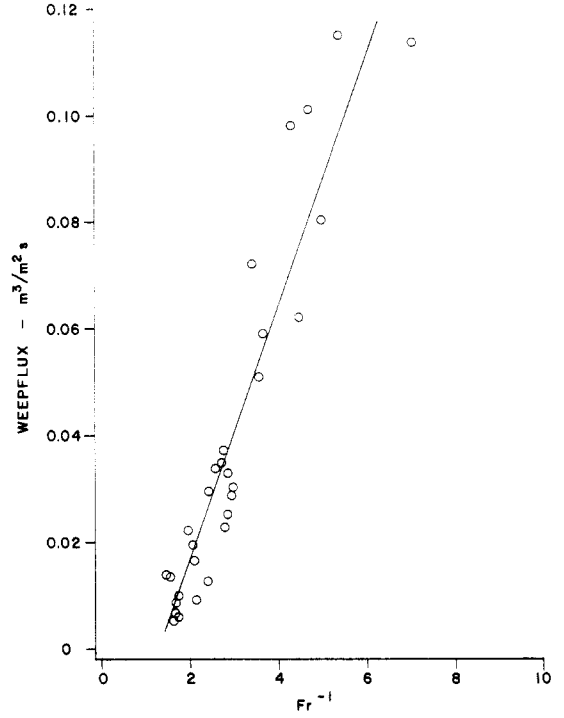

Figure 17. Correlation of results for tray D (6.4-mm holes, 10.2%): air–water.

Figures 16–21 show correlated results for each individual tray and system used, and they are combined in Figure 22. We have omitted results where the weeping rate divided by the total liquid rate (the weep fraction) was greater than 0.5, because under these conditions, the tray operated extremely nonuniformly, with some areas totally bubbling and others totally weeping. The implicit model on which our correlation is based is one of uniform weeping, and this certainly breaks down at very high values of the weep fraction. All the results may be reasonably brought together by using the proposed method of correlation, except perhaps those for the tray with 3 mm diameter holes

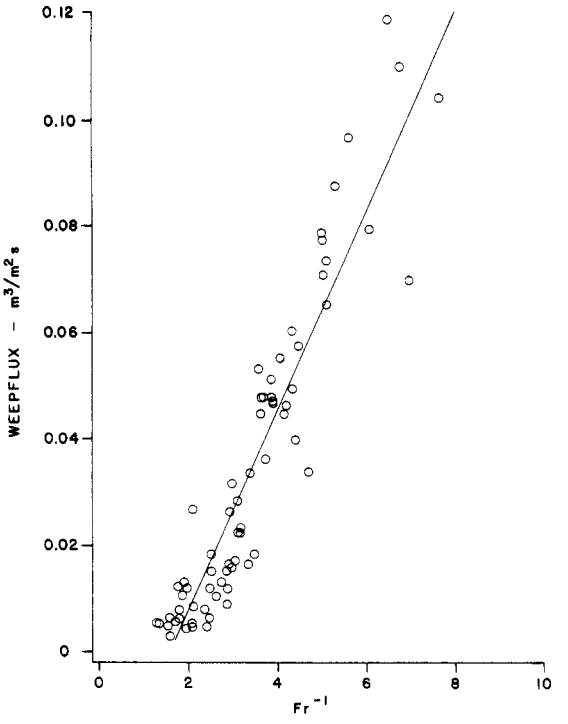

Figure 18. Correlation of results for tray A (12.7-mm holes, 10.2%): air–water.

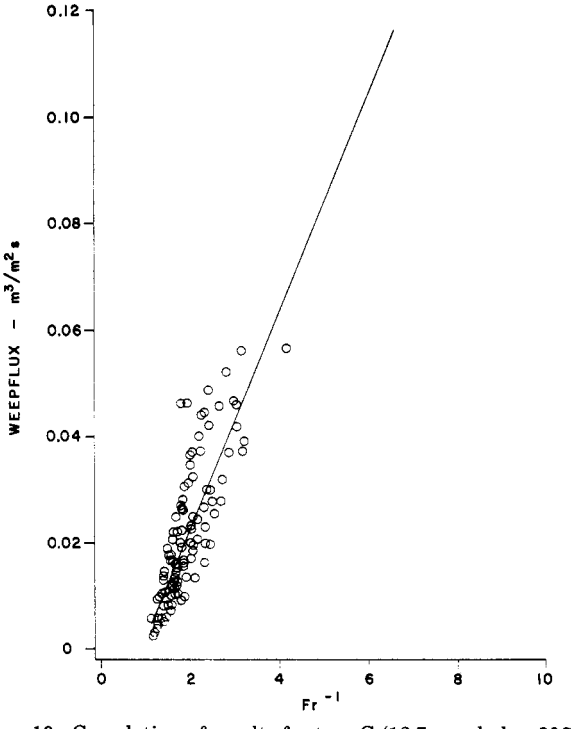

Figure 19. Correlation of results for tray C (12.7-mm holes, 20%): air–water.

(Figure 16). For this tray, weeping was found to be slightly less at high weep rates than for the other trays when compared in this way. The best straight line through the points shown on Figure 22, fitted by linear regression, is

$$WF = 0.020Fr^{-1} - 0.030 \quad (6)$$

Equation 6 can be used to estimate the weep point ($WF = 0$) which occurs when $Fr = 0.67$.

Use of the Weep Rate Correlation. The correlation is used to predict the weep rate by basing U_h on the total hole area. It neglects that some holes may not be bubbling or are partly filled with liquid. We recognize that this is

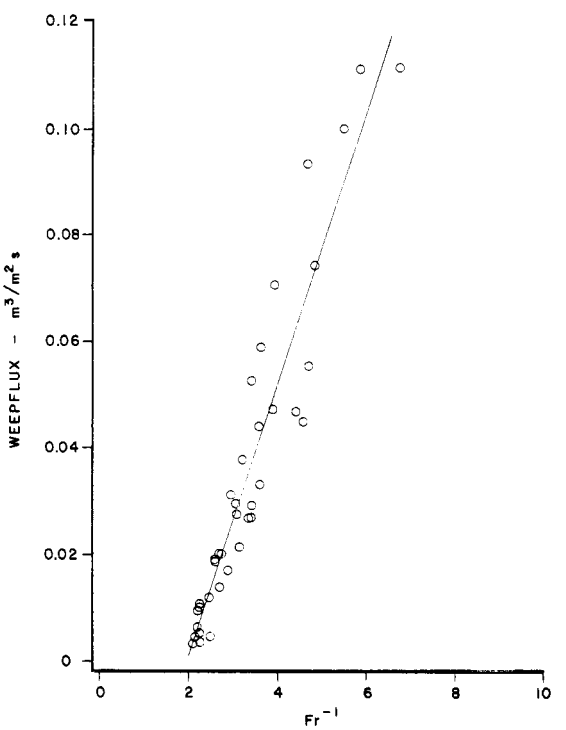

Figure 20. Correlation of results for tray A (12.7-mm holes, 10.2%): air–Isopar M.

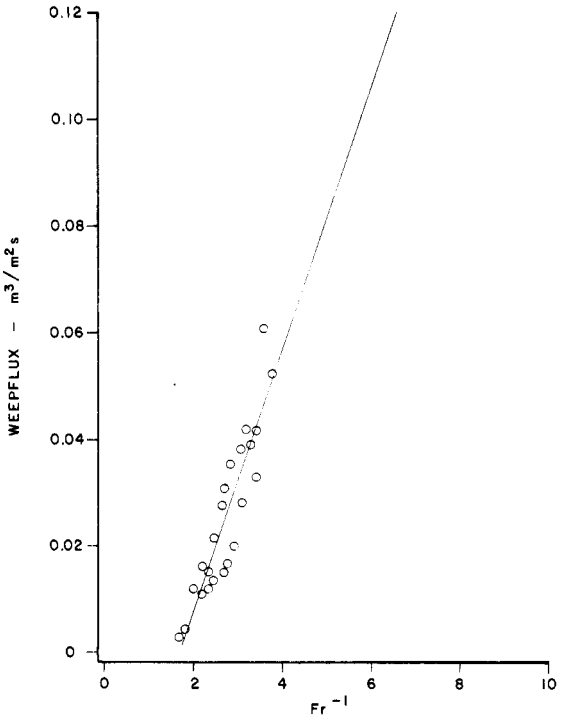

Figure 21. Correlation of results for tray C (12.7-mm holes, 15%): air–Isopar M.

an oversimplification. Unfortunately, more rigorous treatments of the problem (Prince and Chan, 1965), in which the fraction of holes bubbling and weeping are estimated, have not been sufficiently developed to enable them to be used in a practical correlation.

We have found that Colwell's correlation (Colwell, 1981) can be used to estimate h_{CL} under weeping conditions. Two trial-and-error procedures are required. One is inherent in Colwell's method, and also an overall trial-and-error procedure is necessary, as h_{CL} depends on the liquid load over the weir, which in turn depends on the weep rate.

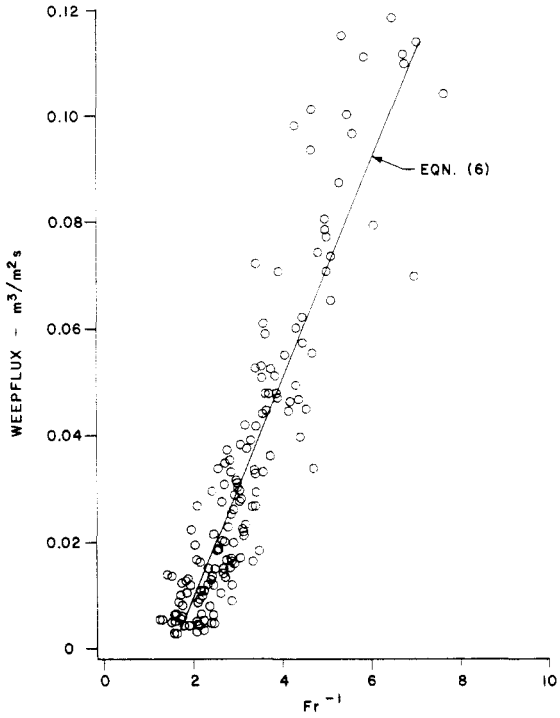

Figure 22. Correlation of all results.

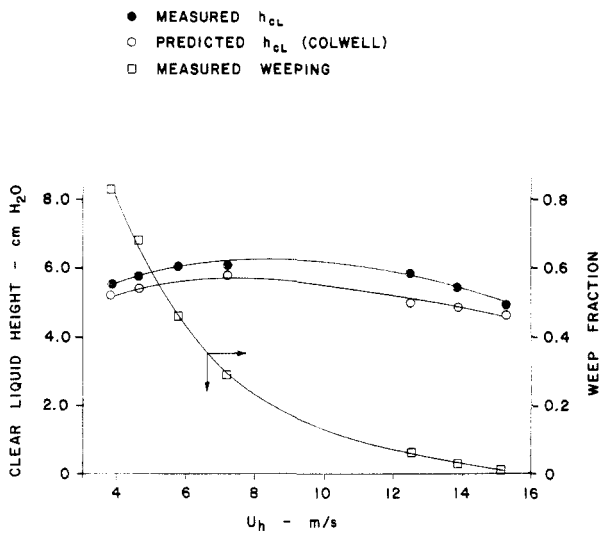

Figure 23. Prediction of clear-liquid height using Colwell's correlation under weeping conditions: tray A, air–water, weir = 75 mm.

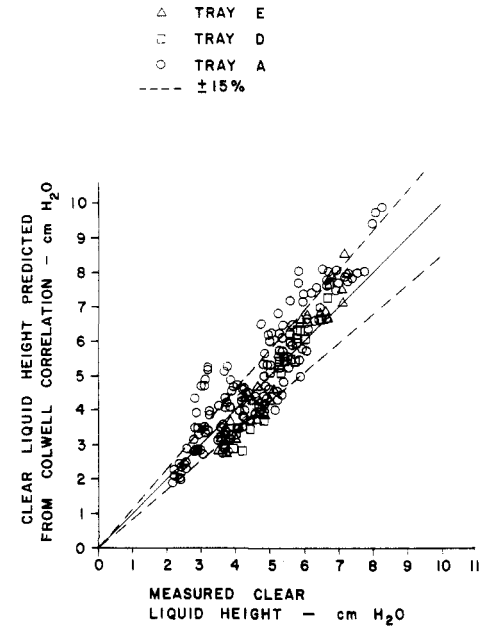

Figure 24. Prediction of clear-liquid height using Colwell's correlation: air–water.

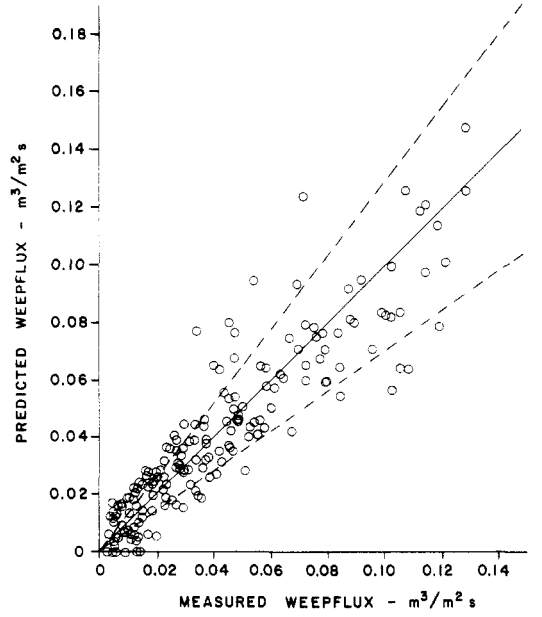

Figure 25. Parity plot of measured vs. predicted weeping flux: trays A, D, and E, air–water and air–Isopar M, ±30% (- - -).

Colwell's correlation was found to be preferable over the correlation of Hofhuis and Zuiderweg (1979) because the latter breaks down completely at the seal point when the liquid load over the weir falls to zero.

A typical example of the prediction of h_{CL} using Colwell's correlation is shown in Figure 23 and for a range of conditions in Figure 24. Note that the maximum in the clear-liquid height with the hole gas velocity in Figure 23 is predicted by the correlation. Figure 25 shows a parity plot of measured weep flux vs. predicted weep flux using (6) and Colwell's correlation for h_{CL}, all for 10% free area sieve trays. We conclude that the correlation reported here can usefully be employed to estimate weep rates. One reservation is that under vacuum distillation conditions, with large diameter trays, the liquid loads are low. Consequently, a very small weep flux corresponds to a significant fractional weep rate based on the liquid flow to the tray. The proposed correlation is inaccurate under these conditions. Another reservation is that the correlation is unsuitable for trays having very small holes, such as are used in air separation.

It is of course recognized that the range of physical properties used in the present work was somewhat limited. Further testing of the proposed correlation is required by using a wider range of gas and liquid properties and also preferably by using distillation systems.

It is of interest to investigate whether other workers' data can be correlated in the way we propose here. Figure 26 shows data of Brambilla et al. (1979) which also appear to be reasonably well-correlated by plotting the weep flux vs. Fr^{-1}. However, the measured weeping rates of Brambilla et al. tend to be rather lower than would be predicted by the present correlation. The reason for this is not known, but it may possibly be attributed to the small column they used (0.52 m × 0.34 m).

Lemieux and Scotti (1969) have published weeping data from a similar size sieve tray to that used in the present work. Weeping rates from one of their trays, which had

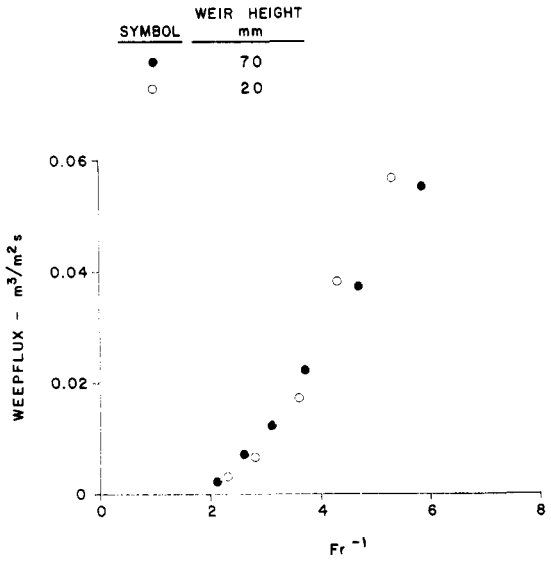

Figure 26. Correlation of Brambilla's weeping data: hole diameter = 10 mm, 14%, liquid rate = 8.7 $m^3/(m\ h)$.

12.7-mm holes, can in principle be compared with the present data. Clear-liquid heights were not reported by Lemieux and Scotti although in some cases they reported the total tray pressure drop so that an estimate of h_{CL} can be made. Unfortunately, it turns out that the weep fluxes reported by Lemieux and Scotti were very low with the result that all their data congregates in the lower left-hand corner when plotted in the way shown in Figures 16–22. In only one case was the weep fraction greater than 0.05. At such low weep fractions, tray behavior is virtually unaffected by the presence of weeping. Consequently, Lemieux and Scotti's data are of little value for comparison with our results. Nevertheless, the general trends of their data are in agreement with those found in the present work. Weeping was found to increase with a reduction in the hole gas velocity and with an increase in the liquid rate. Lemieux and Scotti also found an anomolous effect of the hole diameter, with 25-mm holes weeping more than 12.7-mm holes at low liquid rates but the reverse at high liquid rates.

Conclusion

Equation 6 gives a correlation which can be used to predict weeping rates and hence weep fractions, when used in combination with Colwell's correlation for the clear-liquid height. It has its best accuracy when used for medium-to-heavily liquid loaded trays of small-to-medium diameter. It should not be used when the predicted weep fraction is greater than 0.5. The correlation allows an estimate of tray efficiency under weeping conditions to be made when used in combination with a tray efficiency model published previously (Lockett et al., 1984).

Acknowledgment

Acknowledgement is made to the Shell International Petroleum Co. which provided financial support for S. Banik during this project and to the Exxon Corp. for the gift of the Isopar M. This paper was originally presented at the AIChE Annual Meeting, San Francisco, Nov, 1984.

Nomenclature

Fr = Froude number
g = acceleration due to gravity, m s^{-2}
h_{CL} = clear-liquid height, m
ΔP_d = dry tray pressure drop, m of liquid
ΔP_T = tray pressure drop, m of liquid
U_h = hole gas velocity, m s^{-1}
WF = weep flux, $m^3/(m^2\ s)$

Greek Symbols

ξ = orifice coefficient
ρ_G, ρ_L = gas and liquid densities, kg/m^3

Literature Cited

Banik, S. Ph.D. Thesis, University of Manchester Institute of Science and Technology, Manchester, U.K., 1982.
Brambilla, A.; Gianolio, E.; Nencetti, G. F. *Inst. Chem. Eng. Symp. Ser.* **1979**, *No. 56*, 3.2/1.
Brown, R. S. Ph.D. Thesis, University of California, Berkeley, 1958.
Colwell, C. J. *Ind. Eng. Chem. Process Des. Dev.* **1981**, *20* (2), 298.
Hofhuis, P. A. M.; Zuiderweg, F. J. *Inst. Chem. Eng. Symp. Ser.* **1979**, *No. 56*, 2.2/1.
Koziol, A.; Koch, R. *Inz. Chem.* **1976**, *6* (3), 531.
Lemieux, E. J.; Scotti, L. J. *Chem. Eng. Prog.* **1969**, *65*, 52.
Lockett, M. J. *Trans. Inst. Chem. Eng.* **1981**, *59*, 26.
Lockett, M. J.; Rahman, M. A.; Dhulesia, H. A. *AIChE J.* **1984**, *30* (3), 423.
Nutter, D. E. *Inst. Chem. Eng. Symp. Ser.* **1979**, *No. 56*, 3.2/47.
Nutter, D. E. *AIChE Symp. Ser.* **1972**, *68* (124), 73.
Prince, R. G. H.; Chan, B. K. C. *Trans. Inst. Chem. Eng.* **1965**, *43*, T49.
Wada, T.; Kageyama, O.; Azami, S. *Kagaku Kogaku* **1966**, *30*, 507.
Zenz, F. A.; Stone, L.; Crane, M. *Hydrocarbon Process.* **1967**, *46* (12), 138.
Zhou, Y. F.; Shi, J. F; Wang, X. M.; Ye, Y. H. *Int. Chem. Eng.* **1980**, *20* (4), 642.

Received for review December 4, 1984
Revised manuscript received October 9, 1985
Accepted November 14, 1985